

CHARMED MESON PRODUCTION AND DECAY*

James E. Wiss
Lawrence Berkeley Laboratory
University of California, Berkeley, California 94720

ABSTRACT

We discuss charmed meson production through two body processes in e^+e^- annihilation. Evidence for states of charm excitation beyond the D^* is obtained through an analysis of the recoil spectrum against D 's produced at $E_{cm} = 4.415$ GeV. Direct observation of the reaction $D^{*+} \rightarrow \pi^+ D^0$ in SPEAR data taken at E_{cm} exceeding 5 GeV will then be discussed. This reaction provides an extremely accurate determination of the D^{*+}, D^0 mass difference ($M_{D^{*+}} - M_{D^0} = 145.3 \pm 0.5$ MeV/ c^2) and a new upper limit on $D^0 - \bar{D}^0$ mixing effects. The results of fits to the D^0, D^+ recoil spectrum will then be discussed. These fits provide considerable information on the masses, production mechanisms, and decays of charmed mesons. This will be followed by a brief presentation of the known cross sections for charmed meson production and decay and an analysis of possible resonant structure in the decay products of the D^0 and D^+ . Lastly, we discuss a bubble chamber D^0 candidate submitted by Hagopian et al., of Florida State University.

PRESENTATION OF CHARM SIGNALS

Much of this talk describes data from the SLAC-LBL collaboration's experiment on e^+e^- annihilation conducted at the Magnetic Detector at SPEAR. Fig. 1 shows a schematic of the Magnetic Detector. Momentum measurement is afforded by system of two proportional chambers and four wire spark chambers which cover the polar angle region $|\cos\theta| < 0.65$. Momentum resolution is approximately 1.2% at 1 GeV/c. Particle identification is achieved using time-of-flight information provided by a cylinder of 48 scintillation counters placed at a radius of 1.5 m. This system has a R.M.S. time resolution of 0.35 ns over a flight path of 1.5 to 2.0 m.

Unless otherwise stated, the data sample consists of 29,000 hadronic events ($L = 1830$ nb $^{-1}$) collected in a non-uniform scan from 3.9 to 4.6 GeV center-of-mass energy (E_{cm}), and two high statistics, monoenergetic samples collected at $E_{cm} = 4.028$ GeV and $E_{cm} = 4.415$ GeV of luminosity $L = 1280$ nb $^{-1}$ and 1630 nb $^{-1}$ respectively. The scan data was the data set in which charm was originally discovered.¹ Subsequent to that result, the SLAC-LBL collaboration

*This work was done with support from the U.S. Energy Research and Development Administration under the auspices of the Division of Physical Research.

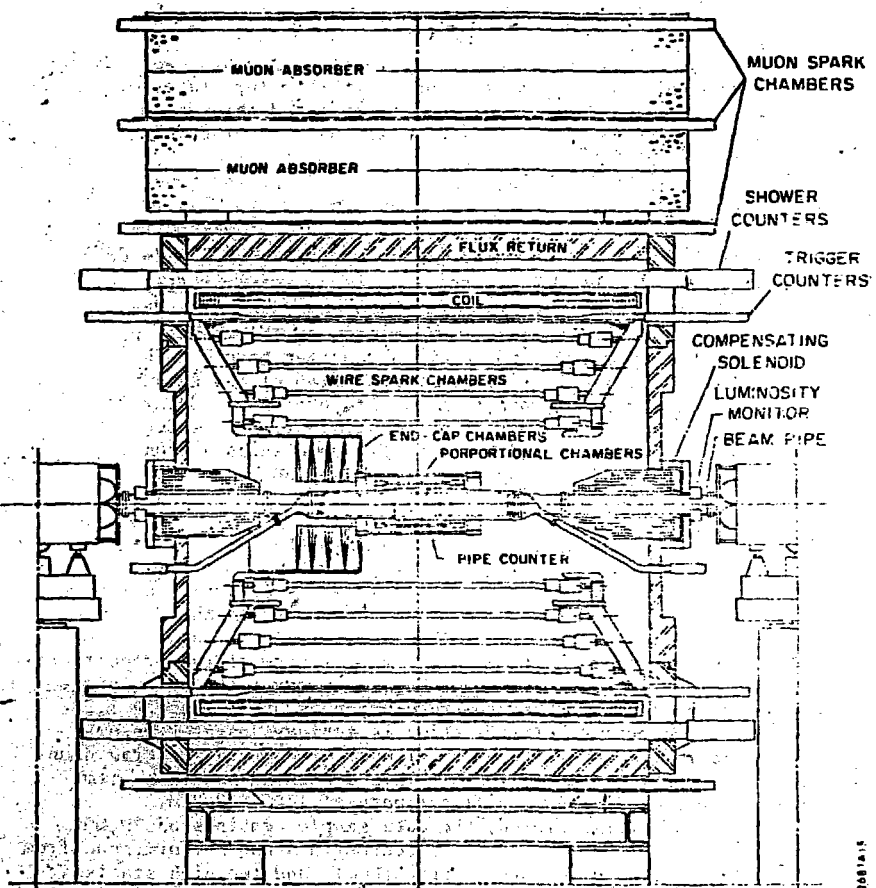
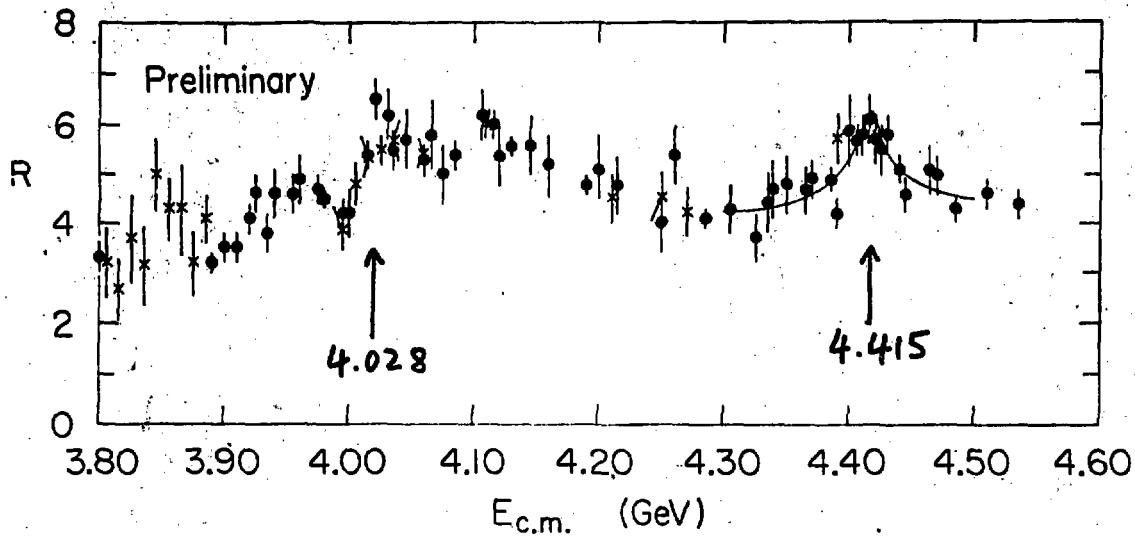


Fig. 1
Diagram of the Mark I SLAC-LBL
Magnetic Detector.



XBL 767-8808

Fig. 2

Plot of $R = \sigma_{Had} / \sigma_{\mu\nu}$ as a function of center-of-mass energy. Much of the data reported on here was taken at the two marked locations.

devoted a considerable portion of their remaining running to collection of data at the two most prominent peaks in the $R = \sigma_{\text{Had}}/\sigma_{\mu\mu}$ plot shown in Fig. 2.

Fig. 3 shows the $K\pi\pi$, $K\pi\eta$, and $K\pi$ invariant mass distribution for the complete data with $E_{\text{cm}} = 3.9$ to 4.6 GeV. Each signal has a width compatible with the resolution of its particular channel. In Fig. 4 we present evidence for a $K_S^0\pi^+\pi^-$ decay mode for the new neutral meson. The kaons of Fig. 3 are selected by a simple track identification algorithm based on time-of-flight information. The measured time-of-flight for a given track is compared to the flight time expected under the pion and kaon hypothesis. The expected flight time is computed from the measured momentum and reconstructed flight path. To be tagged as a kaon, the track must have a flight time more consistent with the kaon hypothesis than the pion hypothesis, and the χ^2 for that hypothesis cannot exceed 3. If either requirement is violated, or no time-of-flight information is available, the prong is tagged as a pion.

The K_S^0 's of Fig. 4 are selected by an invariant mass cut coupled with a geometric, vertex cut.

Before discussing the recoil system against these new mesons, we briefly list the evidence linking these particles to the (D^0, D^+) charmed isodoublet. As previously mentioned, the new mesons were discovered in e^+e^- annihilation near 4.1 GeV center-of-mass energy. If one interprets the psion family--the ψ , ψ' and ψ'' (4.415)--as $c\bar{c}$ bound states, this would be prime hunting ground for the charmed mesons. One would expect to find charmed mesons right after the onset of the last narrow resonance of the psion, i.e. directly after the ψ' .

The true earmark of charm is a tendency for charmed isodoublet states to decay into final states containing a kaon. We see that all three of the neutral meson's observed decay modes involve kaons. The observed decay mode of the charged meson into $K^-\pi^+\pi^+$ provides a particularly dramatic demonstration of the GIM mechanism which causes charmed mesons to decay into kaons. Here the Cabibbo enhanced decay modes for a state of positive charge and charm are into states of negative strangeness. Such final states are labeled exotic, since, if they were due to the strong decay of a new state, the state could not be constructed from a quark-anti quark pair of the conventional u, d, s quarks. As we shall demonstrate shortly, both the charged and neutral states appear to have states of equal or greater mass recoiling against them. Such associated production would be required for a state possessing a new quantum number conserved by the electromagnetic (and strong) interaction. Lastly, a study of the $K^+\pi^+\pi^0$ Dalitz plot provides evidence for parity violation in the decays of the new mesons, by much the same reasoning as the τ - θ puzzle of the mid 50's.³

Having presented a quick review of the evidence linking the new mesons to the (D^0, D^+) charmed isodoublet, we will assume that identification throughout the remainder of this talk.

A QUALITATIVE LOOK AT THE RECOIL SPECTRUM AGAINST CHARMED MESONS

In Fig. 5a, b, and c we show the recoil spectrum against the $(K_S^0)^0$ (1865), the $(K^0\pi)^0$ (1865), and the $(K^0\pi)^{\pm}$ (1875) for the data

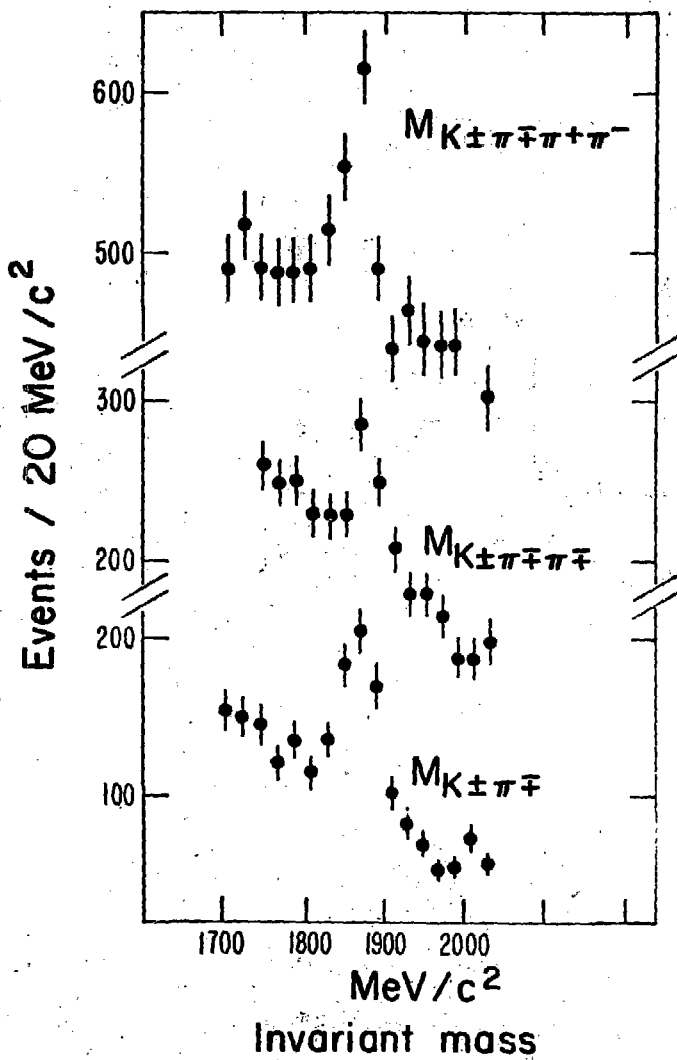


Fig. 3

Three charmed signals for the energy range $3.9 < E_{c.m.} < 4.6$ GeV.

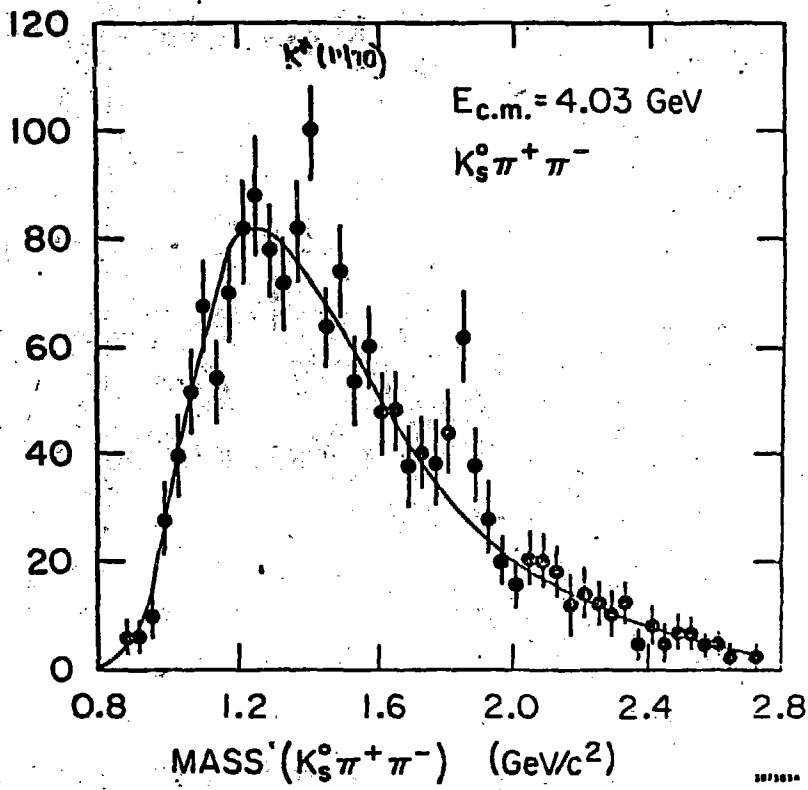


Fig. 4

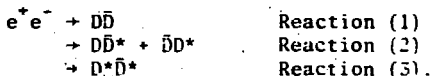
Evidence for a $K_S^0 \pi^+ \pi^-$ decay mode of the D^0 . Y - ordinate is in units of Events per 40 MeV/c^2 . Data was collected at $E_{cm} = 4.028 \text{ GeV}$.

collected from $E_{cm} = 3.9$ to 4.6 GeV. In Fig. 5 we require the $K^{\pm}\pi^{\mp}$ and $K^{\mp}\pi^{\pm}\pi^{\mp}$ invariant mass to lie from 1820 to 1900 MeV/c^2 , and require the $K^{\mp}\pi^{\pm}\pi^{\pm}$ invariant mass to lie from 1850 to 1910 MeV/c^2 . All three spectra are subtracted spectra, computed with a fixed D^0 mass of 1865 MeV/c^2 . For the neutral meson, the backgrounds are taken from adjacent regions of the $K\pi$ and $K3\pi$ invariant mass plots, while for the $K2\pi$, D^+ signal, we use a background taken from the non-exotic $K\pi\pi$ system subject to identical cuts in invariant mass.

Approximately 60% of the legitimate $D^0 \rightarrow K^-\pi^+$ candidates will be classified as $\pi\bar{\pi}$ or $K\bar{K}$ by the time-of-flight tagging system, owing to our finite time-of-flight resolution. Experimentally, such misidentified D^0 candidates can be easily found because they create narrow reflection peaks in the $K\bar{K}$ and $\pi\bar{\pi}$ invariant mass plots. Except for negligible differences in the energy loss corrections for pions vs. kaons, the D^0 momentum will be correctly measured for these reflection D^0 candidates. Thus they can be easily entered in a recoil mass distribution if the recoil mass is computed with a fixed D^0 mass.

All three recoil spectra show evidence for sharp recoil peaks, indicating that charm production occurs primarily through two-body production processes for the energies under discussion. These peaks appear at nearly the same recoil mass for all three signals, but the area ratios are quite different for the charged versus the neutral recoil system.

The peaks shown in Fig. 5 appear to represent charmed meson production via the neutral and charged versions of:



For D masses near 1870 MeV/c^2 and D^* masses near 2010 MeV/c^2 one expects reflection peaks due to reactions 2 and 3 to lie at 2010 and 2150 MeV/c^2 respectively.

The sharpness of the peak ascribed to $D^*\bar{D}^*$ production indicates that D^* 's can cascade to D 's via pion emission as expected for a pair of mesons which carry a common conserved quantum number. A quantitative analysis of the recoil spectrum, which we shall discuss later, shows evidence for $D^{*0} \rightarrow D^0\gamma$ as well, occurring at a rate comparable to $D^{*0} \rightarrow \pi^0 D^0$.

In Fig. 6a we present the " $K\pi$ " recoil spectrum for data collected at $E_{cm} = 4.028$. The solid curve of Fig. 6a gives the expected shape of the D^0 recoil system for Reactions (2) and (3) where $D^{*0} \rightarrow D^0\pi^0$. We have computed this curve using a nominal D^0, D^{*0} mass of 1865 and 2005 MeV/c^2 and have adjusted the peak areas to crudely match the data.

The interpretation of the second peak near 2150 MeV/c^2 as a kinematic reflection of Reaction (3) may appear surprising in light of its narrow width. An alternative interpretation is that this peak is due to the production of a higher mass charmed state at 2150 MeV/c^2 . This interpretation is contradicted, however, by the data of Fig. 6b, which shows the D^0 recoil spectrum at $E_{cm} = 4.415$ GeV. The solid curve again gives the positions of peaks due to Reactions (2) and (3). We note that the peak that was at 2150

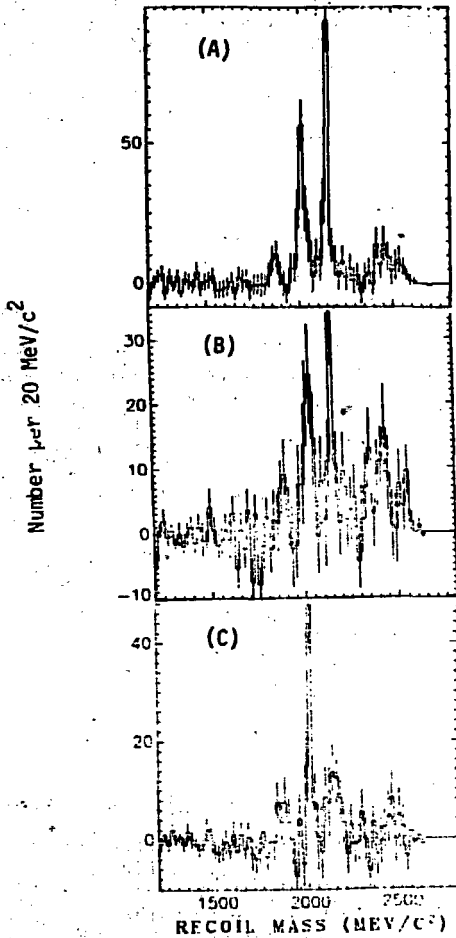


Fig. 5

Subtracted recoil mass spectra against D^0 's and D^+ 's for the data from $3.9 E_{cm} = 4.6 GeV$.

- A) Recoil mass against the $K\pi$ (1865)
- B) Recoil mass against the $K3\pi$ (1865)
- C) Recoil mass against the $K2\pi$ (1875)

Spectra are computed using the indicated nominal fixed masses.

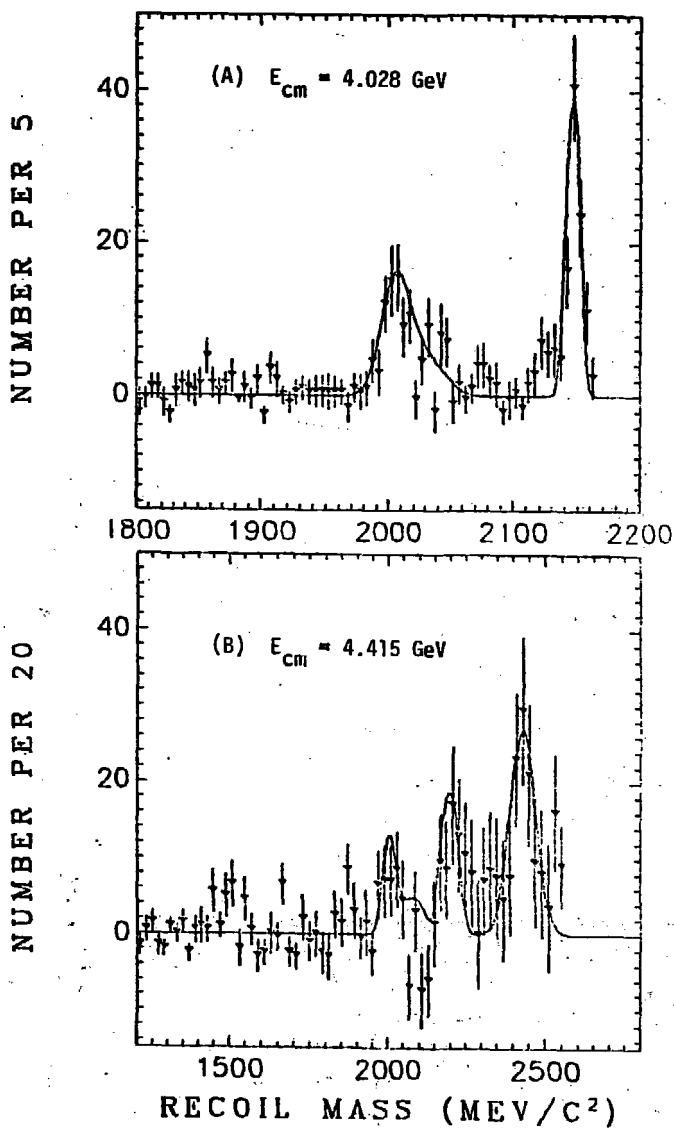


Fig. 6
 D^0 subtracted recoil spectra at two fixed energies. Solid curves are explained in text.

MeV/c² in Fig. 6a has shifted to 2200 MeV/c². This is what would be expected for a reflection of Reaction (3), whereas a new resonance at 2150 MeV/c² would not be expected to change position when the center-of-mass energy changes.

We note the presence of an enhancement at 2440 MeV/c² in the recoil spectrum obtained at E_{cm} = 4.415 GeV. The solid curve of Fig. 6b represents this enhancement by a Gaussian peak centered at 2440 MeV/c² with a width of $\sigma = 50$ MeV/c². Such an enhancement may be due to multibody charm production such as $e^+e^- \rightarrow D^*\bar{D}^*\pi$, or the formation of a new, higher-mass charmed state. Higher mass states are expected in the charm theory, but since this enhancement can be tolerably fit by a multiparticle phase space Monte Carlo, we cannot prove that such new states exist.

DIRECT OBSERVATION OF $D^{*+} \rightarrow D^0\pi^+$

Up to this point, our evidence for the existence of the D^* comes through the observation of structure in the D^0 and D^+ recoil spectra. In this section we will present direct evidence for the existence of the D^{*+} by constructing its invariant mass from the $K^-\pi^+\pi^+$ final state obtained via the sequence $D^{*+} \rightarrow \pi^+D^0$; $D^0 \rightarrow K^-\pi^+$. Because of the low Q value for the reaction $D^{*+} \rightarrow \pi^+D^0$, the cascade pion essentially moves in the Magnetic Detector Frame with the same velocity as the D^{*+} , and hence has only 7% of the D^{*+} momentum [i.e. $P_{\pi^+} = (M_{\pi^+}/M_{D^{*+}})P_{D^{*+}}$]. Because of the 4 kG magnetic field of the SPEAR Magnetic Detector, particles having momentum less than ≈ 70 MeV/c will escape detection; hence, in order to observe the π^+ from $D^{*+} \rightarrow \pi^+D^0$, one must operate where D^{*+} momenta exceed 1 GeV/c². For this reason, the data reported in this section come from data collected at center-of-mass energies from 5 to 7.8 GeV. This sample represents a total integrated luminosity of 17,000 nb⁻¹.

Figure 7 shows the $K\pi$ invariant mass distribution for neutral $K\pi$ pairs with $K\pi$ momentum exceeding 1.5 GeV/c. In this analysis we employ a previously described time-of-flight weighting algorithm¹ rather than the track tagging algorithm described in the first section. Under this weighting technique, each track is assigned weight for being a pion, kaon, and proton, computed from the measured time-of-flight T^M and the time-of-flight expected T_i^E from the measured momentum and flight path under the given mass hypothesis. The weight is computed via the expression

$$W_i = \exp \left[\frac{1}{2} \left(\frac{T^M - T_i^E}{.35 \text{ ns}} \right)^2 \right]$$

with W_i normalized such that: $\sum_{i=\pi K p} W_i = 1$. One can then construct

histograms, say the $K\pi$ invariant mass histogram, by entering a given neutral two-prong combination with a weight given by $W_K^1 W_\pi^2$. The same two-prong combination will enter the histogram again under the assumption that particle 2 is the kaon and particle 1 is the pion with a new weight $W_\pi^1 W_K^2$.

We see clear evidence for high momentum D^0 production in the data of Fig. 7. In fact the signal to background ratio is improved

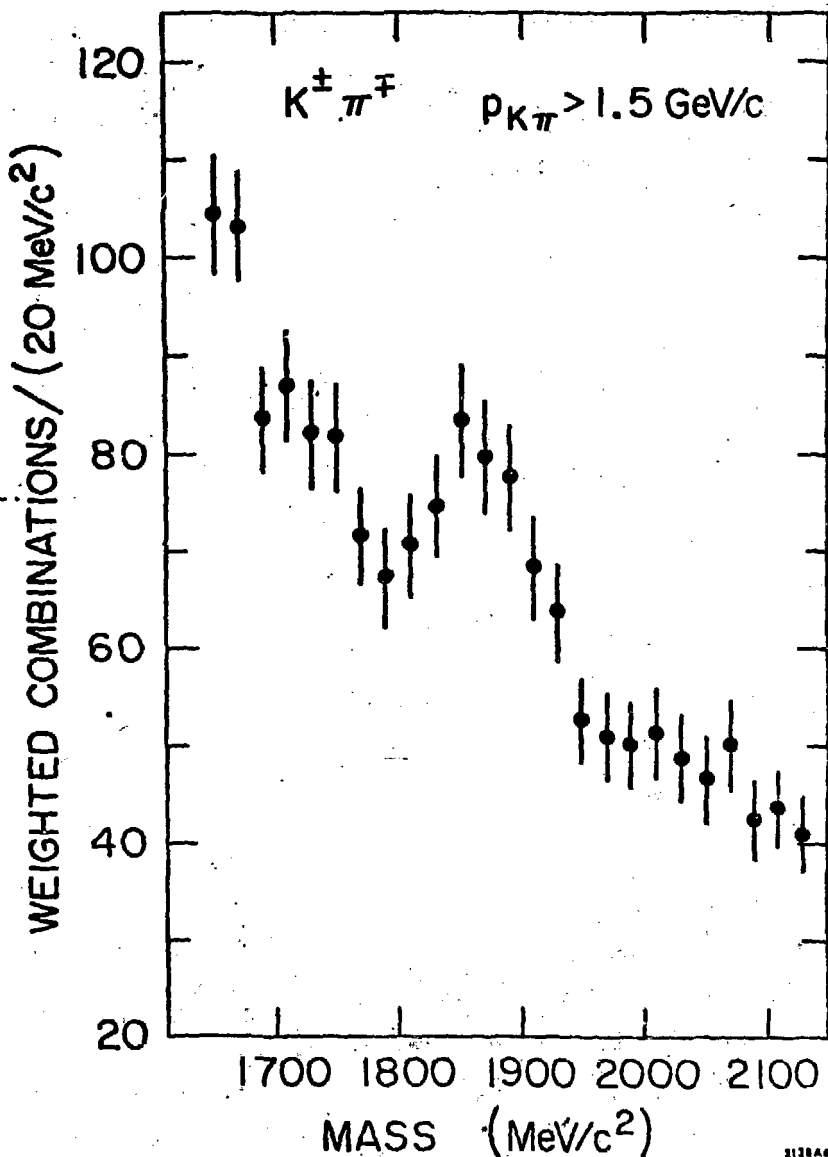


Fig. 7

D⁰ signal in data collected above
E_{cm} = 5 GeV. Here we require p_D > 1.5
GeV.

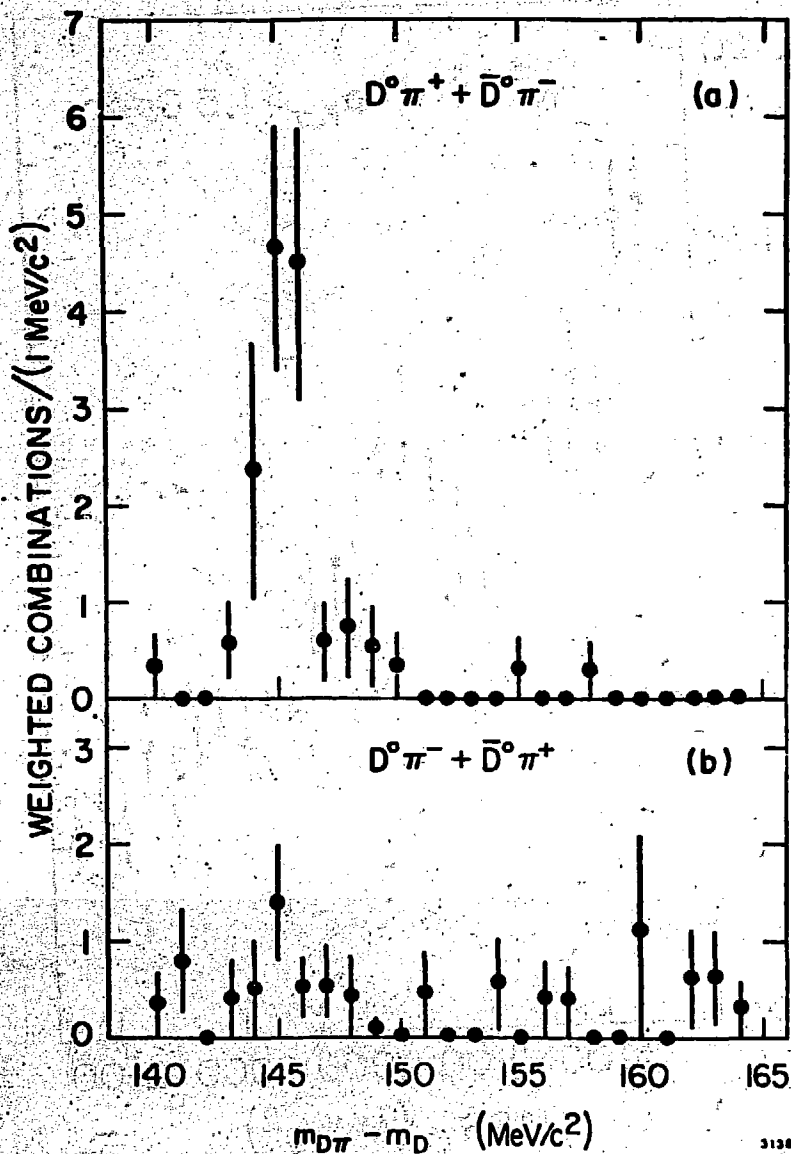


Fig. 8

D^{*+}, D^0 Mass difference plot. D^0 's are selected by requiring their invariant mass to lie from 1820 - 1910 MeV/c².

by requiring $P_{K\pi} > 1.5$ GeV. The signal of Fig. 7 is considerably broader than that of Fig. 3. This broadening is due to the effects of $K\pi$ interchange in the calculation of the $K\pi$ invariant mass. For D^0 's with momenta exceeding 1.5 GeV/c² such $K\pi$ interchange can shift the computed $K\pi$ invariant mass by over 200 MeV/c².

In Figs. 8a and b we show the $D^0\pi^+$ and $D^0\pi^-$ invariant mass plot. Because the calculation of $M_{D^0\pi^\pm}$ is dominated by the mass that one assumes for the D^0 , we plot $M_{D^0\pi^\pm} - M_{D^0}$ rather than $M_{D^0\pi^\pm}$. For this plot we require a D^0 candidate to have a $K\pi$ invariant mass from 1820 to 1910 MeV/c². This mass cut is considerably narrower than the signal seen in Fig. 8 and hence tends to exclude D^0 candidates with transposed pion and kaon. A clear peak is seen in the $D^0\pi^+$ mass difference plot (Fig. 8), at a $M_{D^0\pi^+} - M_{D^0}$ value of 145.3 ± 5 MeV/c². Using a nominal D^0 mass value of 1865 MeV/c² we find this peak corresponds to a D^{*+} mass of 2010 MeV/c². We also see that the signal resides in essentially three 1 MeV/c² bins. The width of the signal is completely consistent with the resolution of the magnetic detector and serves to set an upper limit on the natural width of the D^{*+} (and D^0) of $\Gamma < 2.4$ MeV/c² (90% CL). By comparing the amount of D^0 signal in Fig. 8a with the number of events in the peak of Fig. 7, and taking into account the $D^0\pi^+$ detection efficiency, we estimate that $25 \pm 9\%$ of all D^0 's produced with E_{cm} from 5 to 7.8 GeV and having momentum exceeding 1.5 GeV come from the feed-down process $D^{*+} \rightarrow \pi^+ D$.

LIMITS ON D^0 - \bar{D}^0 MIXING EFFECTS

The observation of a strong D^{*+} signal in the $D^0\pi^+$ invariant mass distribution of Fig. 8a, and its absence in the $\bar{D}^0\pi^+$ invariant mass plot of Fig. 8b, can be used to set limits on the presence of possible D - \bar{D} mixing effects, a topic realizing considerable popularity in the literature. Barring the presence of first-order, neutral $|\Delta C| = 2$, weak currents, mixing would proceed via virtual Cabibbo suppressed intermediate states, such as $D^0 \rightarrow \pi^+\pi^- \rightarrow \bar{D}^0$, and hence mixing amplitudes would be on the order of $\tan^2 \theta_{Cabibbo}$. If, on the other hand, first order $|\Delta C| = 2$ neutral currents existed, D^0 - \bar{D}^0 mixing might be nearly complete (i.e. the characteristic time it would take a D^0 to mix into a \bar{D}^0 would be considerably shorter than the D^0 lifetime).

The data of Fig. 8 clearly rule out complete mixing where one would expect to see many charged D^{*+} 's in a $\pi^+K^+\pi^-$ (1865) plot as in a $\pi^-K^-\pi^+$ (1865) invariant mass histogram. A quantitative measure of the possible mixing effects is provided by the mixing ratio which we define as:

$$F_M = \frac{N(D^{*+} \rightarrow \underline{K^+\pi^-\pi^+})}{N(D^{*+} \rightarrow \underline{K^+\pi^-\pi^+}) + N(D^{*+} \rightarrow \underline{K^-\pi^+\pi^+})}$$

where the underlined particles are required to be consistent with D^0 's (or \bar{D}^0 's). We find 38 events within ± 2.5 MeV of the peak in Fig. 8a and 11 events within the peak of Fig. 8b. Here we count any combination with a weight greater than 0.1 as an event. After imposing the additional time-of-flight requirement that the probability

that the K and π , comprising the D^0 or (D^{*0}), have been correctly identified is at least three times the probability that they have been interchanged; the 38 events drop to 26 events, but the 11 events drop to only 3. These later 3 events are consistent with coming from unknown background and instrumental effects. We expect 1.4 events from background (i.e. uncorrelated) particle combinations and 0.6 events from residual $K\pi$ interchange. Thus at the 90% confidence level we find $F_M < 16\%$.

It is of interest to compare this measurement of D^0 - \bar{D}^0 mixing effects to an early measurement reported by Goldhaber,⁷ based on the limits for apparent strangeness violating events involving $K\pi$ (1865) production. Using the time-of-flight particle tagging technique discussed earlier, we find 77 events in our total data sample $3.9 < E_{cm} < 4.6$ GeV with a $K\pi$ (1865) candidate and an additional kaon in the recoil system. These kaons have the opposite charge in 62 of our 77 events, and like charge in 15 of the events. After correcting for the 39% background underneath the $K\pi$ signal we find that in 12±9% of the two kaon events containing a D^0 the two kaons have like charge. This value is 4.2 standard deviations away from 50%, the value expected for complete D^0 - \bar{D}^0 mixing. One expects a like charge ratio of 13% from time-of-flight particle misidentification, as determined by a Monte Carlo simulation predicated on no D^0 - \bar{D}^0 mixing. After correcting for the effects of track misidentification, we find that less than 18% of events containing a D^0 exhibit strangeness violation at the 90% confidence level.

The exact relationship between these two measures of D^0 - \bar{D}^0 mixing depends in detail on the mechanisms for D^0 production over the data sample employed to measure the apparent strangeness violation. In particular, certain production mechanisms should exhibit rather striking interference effects as detailed by Kingsly.⁸ Although we have performed a relatively detailed analysis of D^0 production near $E_{cm} = 4.03$ GeV, we lack the data to do this over the full data sample from 3.9 to 4.6. Denoting the violating fraction by F_V , one finds $F_V > F_M$ irrespective of production; hence the upper limit on F_V serves as a conservative independent upper limit on F_M . Using both measurements we deduce $F_M < 15\%$ (90% CL).

We have seen from the foregoing that D^0 - \bar{D}^0 mixing effects can be excluded beyond about the 10% level, and complete D^0 - \bar{D}^0 mixing is ruled out.

RESULTS OF A FIT TO THE D^0, D^{*+} MOMENTUM SPECTRUM AT $E_{cm} = 4.028$ GeV

As previously mentioned, threshold production of both charged and neutral D's appears to proceed through two-body processes involving D^* 's and D^* 's. We have performed several fits of the joint D^0 and D^{*+} momentum spectrum for data collected at the fixed center-of-mass energy of 4028 ± 5.4 MeV. The momentum spectra at fixed beam energy convey essentially the same information as the recoil spectra presented earlier, but offer the advantage of nearly uniform resolution. Monte Carlo calculations indicate that the $D^0 \rightarrow K\pi$, and $D^{*+} \rightarrow K2\pi$ momentum resolution is ~ 18 MeV/c and varies by $\pm 10\%$ over the full momentum range considered here. The individual D and D^{*+} efficiency variation is also about $\pm 10\%$.

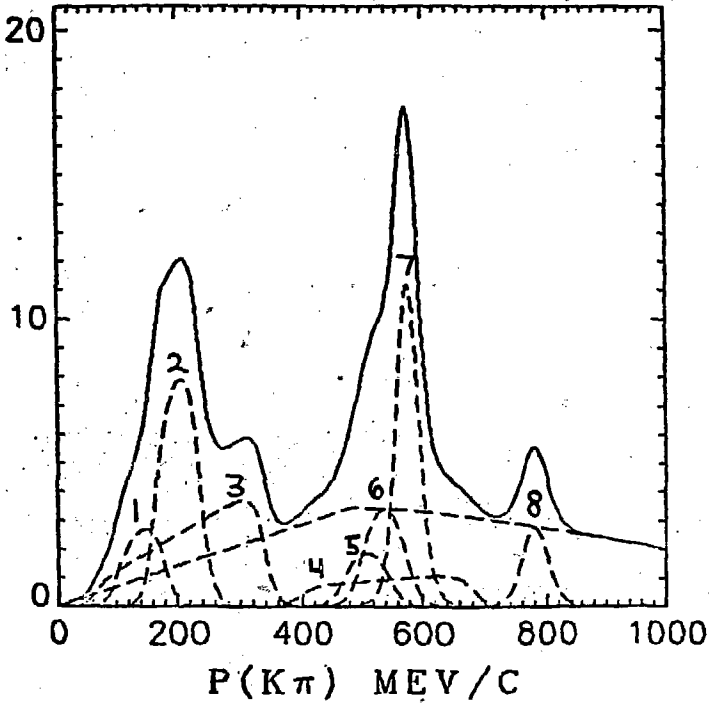


Fig. 9
Illustration of contributions to D^0 momentum spectrum at $E_{cm} = 4.023$ GeV

- | | | |
|-----------------------------------|---------------------------------|-----|
| $e^+e^- \rightarrow D^{*+}D^{*-}$ | $D^{*+} \rightarrow \pi^+D^0$ | (1) |
| $D^{*0}\bar{D}^{*0}$ | $D^{*0} \rightarrow \pi^0D^0$ | (2) |
| $D^{*0}\bar{D}^{*0}$ | $D^{*0} \rightarrow \gamma D^0$ | (3) |
| $D^{*0}\bar{D}^0$ | $D^{*0} \rightarrow \gamma D^0$ | (4) |
| $D^{*+}D^-$ | $D^{*+} \rightarrow \pi^+D^0$ | (5) |
| $D^{*0}\bar{D}^0$ | $D^{*0} \rightarrow \pi^0D^0$ | (6) |
| $\bar{D}^{*0}D^0$ | Direct D^0 | (7) |
| $D^0\bar{D}^0$ | Direct D^0 | (8) |

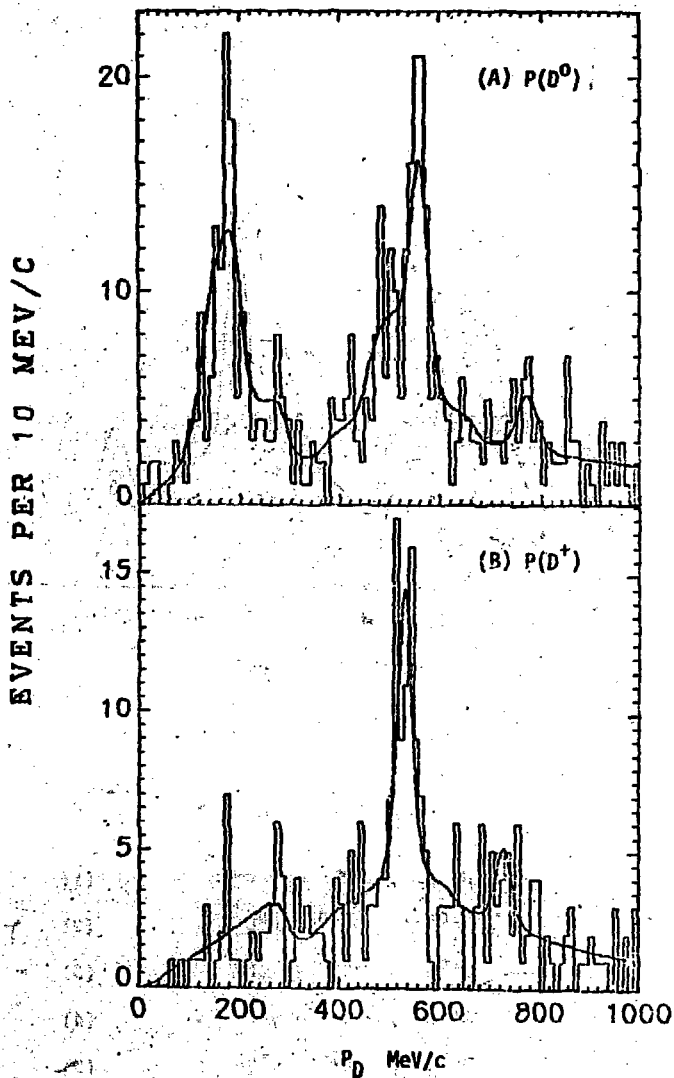


Fig. 10

Results of the simultaneous fits to the D^0 , D^+
momentum spectrum at $E_{cm} = 4.028$ GeV

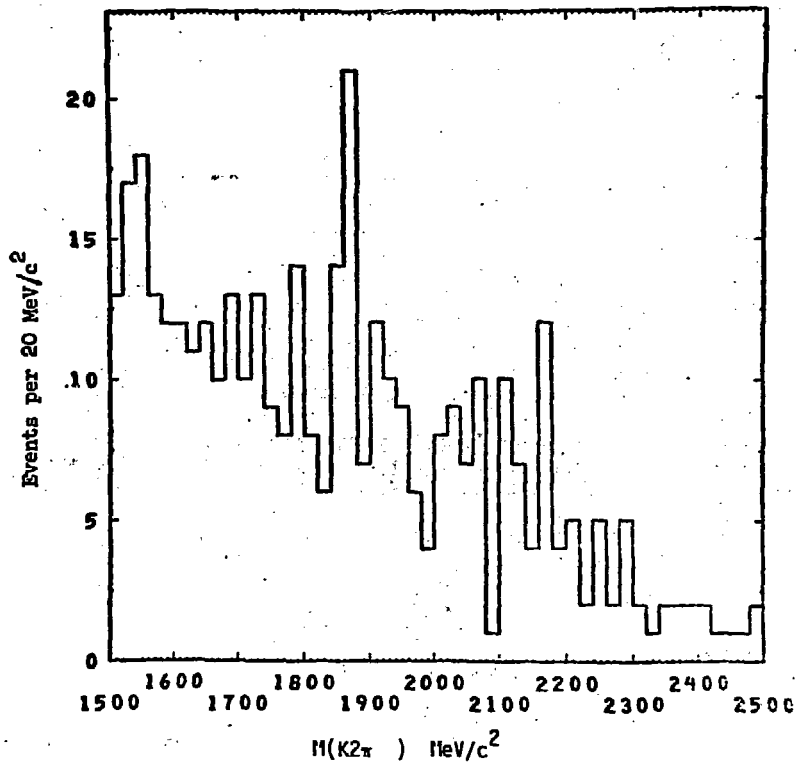


Fig. 11

Demonstration that there are D^+ candidates with momentum less than 320 MeV/c in the $E_{cm} = 4.028$ data. We are plotting the $K\pi$ invariant mass distributions where $P(K\pi) < 320 \text{ MeV}/c$.

We have fit the D^0 and D^+ spectra in terms of neutral and charged versions of reactions 1-3. Implicit in these fits is the assumption of charm conservation; hence D^{*0} 's decay into D^0 's via $D^{*0} \rightarrow \gamma D^0$ and $D^{*0} \rightarrow \pi^0 D^0$. We allow D^{*+} to decay via the processes $D^{*+} \rightarrow \pi^+ D^0$ and $D^{*+} \rightarrow \gamma D^+$. The expected spectral contributions of Reactions 1-3 with these D^* to D decay mechanisms is seen in Fig. 9. These spectral shapes are computed from the known D^* , D^0 momentum resolution and assume isotropic D^* to D decays when the angular distributions are not known to be different. Fig. 9 is meant to be primarily illustrative; we have moved several of the fit parameters within their errors in order to clearly show the contributions of all processes. We employ the constraint that $M_{D^{*+}} - M_{D^0} = 145.3 \pm 5$ MeV/c² in all fits discussed here.

In Fig. 10 we show a comparison of a typical fit to the data. The dashed curve beneath Fig. 10a shows a sideband deduced background. We see that the fit does a reasonably good job in reproducing both the D^0 and D^+ data, although there are some problems with matching the $D^{*0} D^0$ peak's narrow width. This overall agreement shows that two-body production processes appear to dominate D production near threshold. To set an upper limit on multibody D^0 production, we have included a spectral contribution for the process $D^0 \bar{D}^0 \pi^0$. D^0 's from this process will have momentum within a broad peak (FWHM = 200 MeV/c²) centered at 400 MeV/c². As seen in Fig. 10, there is a dip within this region in the data; hence the fit prefers no $D\bar{D}\pi$ contribution and sets a 90% CL upper limit of less than 10% of the D^0 's produced at threshold arising from 3-body processes.

We also see from the data of Fig. 10b the barest hint of a peaked structure near 200 MeV/c. Such a peak could arise from $D^{*+} D^-$ production followed by $D^{*+} \rightarrow \pi^0 D^+$ decay. Clearly the data do not establish this process, but there are indications in the $K\pi\pi$ invariant mass plot for D^+ events with momenta less than 320 MeV/c (see Fig. 11). These events can originate from $D^{*+} D^-$ production followed by either $D^{*+} \rightarrow \gamma D^+$ or $D^{*+} \rightarrow \pi^0 D^+$. The D^0, D^+ momentum fits generally obtain D^{*+} and D^+ masses which are too close to permit the reaction $D^{*+} \rightarrow \pi^0 D^+$, but conclusive evidence for the presence or absence of this decay will have to await new data.

A similar uncertainty in the charged spectrum fit is the importance of the process $D^{*+} \rightarrow \pi^+ D^0$. Quark model considerations indicate that the matrix element for $D^{*+} \rightarrow \gamma D^+$ should be suppressed relative to that for $D^{*0} \rightarrow \gamma D^0$.⁹ This suppression follows from the belief that D^* to D radiative transitions occur via quark spin flip. Generally the light quarks flip, owing to their larger magnetic moment. Thus $D^{*0} \rightarrow \gamma D^0$, involving a flip of the \bar{u} quark of charge $-2/3$, will dominate over $D^{*+} \rightarrow \gamma D^+$, which involves the flip of a charge $1/3$ d quark. Estimates of the suppression range from $1/4$ to $1/25$, depending on the assumed magnitude of the charmed quark magnetic moment.

If these considerations are indeed correct, $D^{*+} \rightarrow \pi^+ D^0$ should be the dominant D^{*+} decay mechanism. Unfortunately the momentum of D^0 's from the process $D^{*+} \rightarrow \pi^+ D^0$ can be quite close (and with present statistics, unresolvable) to D^0 's from $D^{*0} \rightarrow \pi^0 D^0$. For

these reasons we lack precise information on 1) the branching ratios of the D^{*+} into its various decay modes, 2) the relative cross section for the charged versions of reactions 1-3, and 3) the fraction of D^0 's produced at $E_{cm} = 4.028$ GeV due to $D^{*+} \rightarrow \pi^+ D^0$ (estimates range from 6 to 27%).

In the following table we present the firmer results of several D^0, D^{*+} momentum fits:

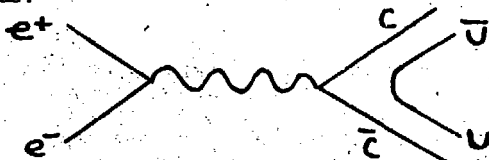
Table I. Results of fits to the D^0, D^{*+} momentum spectrum.

Masses and Br_γ	
$M_{D^0} = 186.3 \pm 3$	$M_{D^{*+}} = 1874 \pm 5$
$M_{D^{*0}} = 2006 \pm 1.5$	$M_{D^{*+}} = 2009 \pm 3$
$\frac{\Gamma(D^{*0} \rightarrow \gamma D^0)}{\Gamma(D^{*0} \rightarrow \text{All})} = (60 \pm 15)\%$	

Relative Production of Neutral 2-Body Processes at $E_{cm} = 4.028$

$\sigma_{D^0 \bar{D}^0}$	\approx	$.48 \pm .12$
$\sigma_{\bar{D} D^0} + \sigma_{D^0 \bar{D}}$	\approx	$.46 \pm .10$
$\sigma_{D \bar{D}}$	\approx	$.06 \pm .03$

The relative $D^0 \bar{D}^0$, $D^{*0} \bar{D}^0$, and $D^0 D^{*0}$ fractions shown in Table I are interesting because they show far more D^{*0} production than one would naively expect from spin statistics and phase space considerations. In models where charm mesons are pair-produced via diagrams such as:



and spin-spin correlations between the u and c quarks are negligible,⁹ one would expect that, aside from the larger number of spin states and smaller phase space available to D^* final states, the $D\bar{D}$, $D\bar{D}^*$, and $D^* \bar{D}^*$ couplings should be universal. In that picture:

$$\frac{\sigma_{D^* \bar{D}^*}}{\sigma_{D^* \bar{D}} + \sigma_{D \bar{D}^*}} \approx g \left[\begin{matrix} 7 \\ 4 \\ 1 \end{matrix} \right] p^3$$

phase space.

The p^3 p-wave angular barrier assumes that the D^* and D have even relative parity and thus all three final states couple to a virtual photon in a p-wave. The factors of 7 : 4 : 1 give the number of available spin configurations, assuming that the D^* is a vector and the D^0 is a pseudoscalar. These are the expected D^* , D spin assignments and they are known to be consistent with our data.¹⁰

Using the tabulated values for the D^{*0} and D^0 masses to compute the p^3 values for the three reactions, we obtain:

$$\begin{array}{rcl} D^{*0} \bar{D}^{*0} & & g_{D^* D^*} \left[\begin{array}{l} 1 \pm 2.7 \\ 17 \pm 1.0 \\ 11 \pm 5 \end{array} \right] \\ \bar{D}^{*0} D^{*0} + \bar{D}^{*0} D^0 & = & g_{D^* D^0} \\ D \bar{D} & & g_{D D} \end{array}$$

from which we find $g_{D^* D^*} : g_{D^* D^0} : g_{D D} = 107 \pm 33 : 5.9 \pm 1.1 : 1 \pm 6$. This result, which rules out $D^* D^0$ coupling, has been noted in several theoretical discussions.¹¹

A final result comes from a fit where we assume that, apart from p-wave angular momentum barriers, $\sigma(D^{*+} D^{*-}) = \sigma(D^{*0} \bar{D}^{*0})$, $\sigma(D^{*+} D^-) = \sigma(D^{*0} \bar{D}^0)$, etc.. This would be true if, for example, the various two-body final states were produced by a pure isosinglet or pure isotriplet intermediate state with no isosinglet-isotriplet interference. Using this assumption, and using theoretical estimates for the $D^{*+} \rightarrow \gamma D^+$ branching ratio, we can obtain the ratio of the $D^{*+} \rightarrow K^+ \pi^-$ over the $D^0 \rightarrow K^+ \pi^-$ branching ratio. We estimate that:

$$\frac{BR(D^{*+} \rightarrow K^+ \pi^-)}{BR(D^0 \rightarrow K^+ \pi^-)} = 1.6 \pm 6.$$

CROSS SECTIONS FOR CHARMED MESON PRODUCTION AND DECAY

In this section we wish to present briefly cross section estimates for the various D^0, D^* decay modes at the fixed energies of $E_{cm} = 4.028$ and 4.415 GeV. Cross section estimation, of course, is an involved process which requires knowledge of the data sample luminosity, an estimate of the detection efficiency for the particular processes under consideration, and a background subtraction algorithm. Luminosity is estimated by counting large-angle bhabha and mu pair events. Efficiencies are estimated through a Monte Carlo program which incorporates the acceptance and triggering conditions of the SPEAR Magnetic Detector. Because we are interested in relatively low multiplicity decays of massive objects, the D detection efficiency is only a mild function of the D momentum, which makes efficiency evaluation relatively model-independent. We have estimated the number of signal events for each process by fitting the appropriate invariant mass plot to a Gaussian signal over a quadratic background. Acceptable fits with low χ^2 were found in each case. The results and their errors which incorporate the uncertainties of each stage of the cross section determination are shown in the following table:

Table II. σ_{Br} for D^0, D^+ decay modes

	4.028	4.415
$\sigma(K^-\pi^+) + \sigma(K^+\pi^-)$	$.52 \pm .12$ nb	$.35 \pm .08$ nb
$\sigma(K^0\pi^+\pi^-) + \sigma(\bar{K}^0\pi^+\pi^-)$	$1.16 \pm .22$ nb	$.78 \pm .24$ nb
$\sigma(K^-\pi^+\pi^+\pi^-) + \sigma(K^+\pi^-\pi^+\pi^-)$	$.92 \pm .25$ nb	$.62 \pm .22$ nb
$\sigma(K^-\pi^+\pi^+) + \sigma(K^+\pi^-\pi^-)$	$.40 \pm .10$ nb	$.33 \pm .12$ nb

The cross sections in the above table are deduced from a fit where we have constrained the three D^0 branching fractions to be equal at $E_{cm} = 4.028$ and $E_{cm} = 4.415$ GeV. The χ^2 of this fit was 1.4 for 2 degrees of freedom. We also note that the entry for $K^0\pi\pi$, which is deduced from $K_S\pi^+\pi^-$, includes corrections for the presence of K_L 's and neutral K_S decay modes.

We conclude from the data of the above table that total D production at 4.028 and 4.415 are equal to within factors of 2. In addition, if charmed meson production accounts for a substantial fraction of the rise in $R = \sigma_{HAD}/\sigma_{\mu^+\mu^-}$ observed at 4.028 and 4.415, we must be observing a small fraction (10%) of the total D production.

RESONANT ANALYSIS OF D DECAY PRODUCTS

Theoretical efforts to understand the D^0 decay multiplicity distribution implied by Table II should take into account possible resonant structure in the D decay products. Our analysis of the $K3\pi$ signal shows that it is compatible with 100% $K\rho$.¹² In Fig. 12 we show the $K3\pi$ invariant mass spectrum for events with at least one dipion within a ρ cut defined from 650 to 850 MeV/c² (Fig. 17a) and both dipions outside the ρ cut (Fig. 12b). Clearly nearly all the $K3\pi$ (1865) signal resides primarily in Fig. 12a and thus contains a dipion satisfying the ρ cut. This ρ cut is narrow in the sense that the $\pi^+\pi^-$ phase space distribution for $D^0 \rightarrow K3\pi$ peaks at 540 MeV/c² and extends from 280 to 1100 MeV/c². After fitting the $K3\pi$ signal to a linear combination of $K\rho$, $K^*\pi\pi$, $K^*\rho$, and $K\pi\pi$ (phase space), we conclude that the fraction into $K\rho$ is $0.85^{+0.11}_{-0.22}$.

There is no evidence for substantial K^* presence, which is somewhat surprising in light of the large amount of ρ . We have also examined the $\rho\pi$ invariant mass plot and can show that $D^0 \rightarrow KA_2$; $A_2 \rightarrow \pi\rho$ does not dominate $K\rho$ production. Unfortunately we cannot rule out $D^0 \rightarrow KA_1$; $A_1 \rightarrow \pi\rho$, since the A_1 Breit-Wigner is quite similar to the $\rho\pi$ phase space for $D^0 \rightarrow K\rho$.

Our analysis of the $D^+ \rightarrow K^-\pi^+\pi^+$ Dalitz plot³ shows that it is consistent with a phase space distribution, and this argues

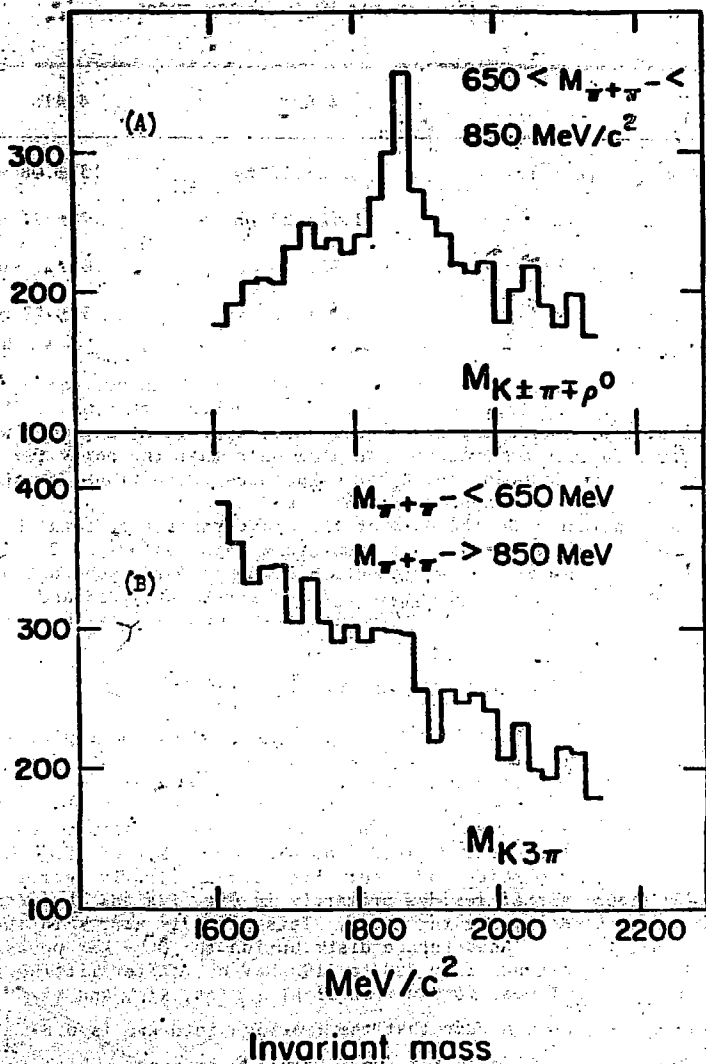


Fig. 12
 Evidence that the $K3\pi$ (1865) is predominately $K\pi\rho$.
 $K3\pi$ invariant-mass plot for events with at least one
 dipion in a ρ band (Fig. 12 A), and with no dipion in a
 ρ band (Fig. 12 B). Note the D^0 signal resides primarily
 in Fig. 12 A.

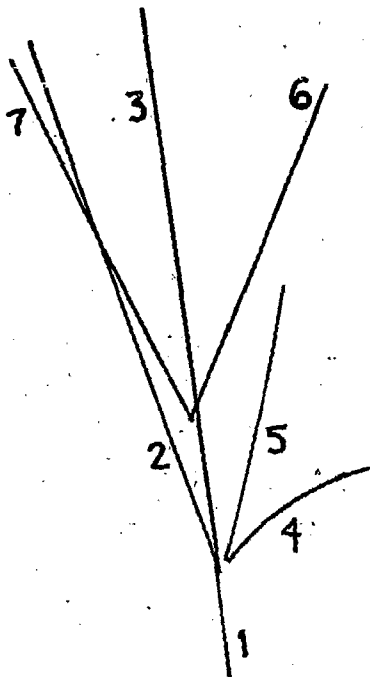


Fig. 13

Schematic of Hagopian et al. bubble chamber event. If tracks 6 and 7 are interpreted as K^+ and π^- they have an invariant mass of $1860 \pm 25 \text{ MeV}/c^2$.

against substantial K^* presence in the D^* three-body decay products as well.

CHARM IN A BUBBLE CHAMBER?

The following section is based on a contributed paper by Hagopian et al.¹³. They find a long-lived $D^0 \rightarrow K\pi$ candidate within a 15 GeV/c π^+ exposure on D_2 . Tracks 6 + 7 of Fig. 13 intersect about 15 cm downstream of the primary vertex at the intersection of tracks 1, 2, and 3. If tracks 6 and 7 are interpreted as a kaon and pion respectively, their invariant mass is $M_{K\pi} = 1860 \pm 25$ MeV/c², which is, of course, consistent with the mass of the SLAC-LBL D^0 candidates discussed earlier. The net momentum of tracks 6 and 7 is 4440 ± 60 MeV/c and appears to point back to the primary vertex. This downstream position and net momentum implies a decay proper time of 2×10^{-10} sec, which certainly indicates the production of a weakly decaying object but is considerably longer than the theoretical D^0 lifetime estimates of 10^{-13} to 10^{-14} seconds.

Charge balance indicates that the initial reaction is pion on proton with a neutron spectator. Uncertainty in the estimation of the missing mass and 4 momentum is primarily due to the unknown fermi momentum of this spectator neutron. Hagopian et al. estimate a missing neutral mass of $M(x^0) = 1120 \pm 150$ MeV/c². When the missing 4 momentum is combined with the 4 momentum of tracks 4 and 5, which appear to form a K_S , one obtains the suggestive mass of $M(K_S x^0) = 1850 \pm 110$ MeV/c². We thus see that there is evidence for associative production. This one event corresponds to a cross section of 10^{-31} on D_2 which is somewhat large when compared to previously published upper limits on hadronic production of charmed mesons. Hagopian et al., however, argue that these experiments may be biased against such long-lived D^0 's.

ACKNOWLEDGEMENTS

It is a pleasure to acknowledge the careful work of my numerous colleagues with the SLAC-LBL Collaboration whose efforts made most of what is reported here possible.

REFERENCES

1. G. Goldhaber et al., Phys. Rev. Lett. 37, 255 (1976).
2. S. L. Glashow, J. Iliopoulos, and L. Maiani, Phys. Rev. D2, 1285 (1970).
3. J. E. Wiss et al., Phys. Rev. Lett. 37, 1531 (1976).
4. G. J. Feldman et al., Phys. Rev. Lett. 38, 1313 (1977).
5. See for example S. L. Glashow and S. Weinberg, Phys. Rev. D15, 1958 (1977); E. A. Paschos, Phys. Rev. D15, 1966 (1977).
6. M. K. Gaillard, B. W. Lee, and J. L. Rosner, Rev. Mod. Phys. 47, 277 (1975).
7. G. Goldhaber, invited talk at the Annual Meeting of the American Physical Society, Chicago. February 1977.
8. R. L. Kingsly, Phys. Lett. 63B, 329 (1976).
9. See for example S. Ono, Phys. Rev. Lett. 37, 655 (1976).
10. H. K. Nguyen et al., submitted to Phys. Rev. Lett.
11. See for example A. De Rujula, H. Georgi, and S. L. Glashow, Phys. Rev. Lett. 38, 317 (1977); M. Suzuki, Phys. Rev. Lett. 37, 1164 (1976).
12. M. Piccolo et al., submitted to Phys. Lett.
13. V. Hagopian et al., Florida State University Report FSU HEP 76-11-29; V. Hagopian et al., Phys. Rev. Lett. 36, 296 (1976).